

The Inhibitory Effect of Docetaxel and p38 MAPK Inhibitor on TZT-1027 (Soblidotin)-induced Antivascular Activity

JUNICHI WATANABE, TSUGITAKA NATSUME and MOTOHIRO KOBAYASHI

*ASKA Pharmaceutical Co. Ltd., Research and Development Division,
Takatsu-ku, Kawasaki-shi, Kanagawa 213-8522, Japan*

Abstract. *Background:* TZT-1027 (Soblidotin), a microtubule (MT)-depolymerizing agent, has antivascular activity through the disruption of microtubules in vascular endothelial cells. Our aim was to elucidate the mechanism of TZT-1027-induced antivascular activity by investigating the impact of various inhibitors. *Materials and Methods:* The inhibitory effects on TZT-1027-induced antivascular activity were evaluated by a tumor perfusion study in mice bearing Colon26 tumors and a vascular permeability study on human umbilical vein endothelial cells monolayer. Western blotting analyses were performed to verify the mechanism of antivascular activity. *Results:* Pretreatment with docetaxel and SB220025, a p38 mitogen-activated protein kinase (MAPK) inhibitor, significantly suppressed the TZT-1027-induced reduction of tumor perfusion and increase in vascular permeability. Gross findings showed that SB220025 visibly attenuated the TZT-1027-induced widespread hemorrhage in tumors. Western blotting analyses revealed that TZT-1027 induced the phosphorylation of p38 MAPK only slightly compared to hydrogen peroxide, and that docetaxel and SB220025 increased the acetylation of α -tubulin an effect opposite to that of TZT-1027. *Conclusion:* TZT-1027-induced antivascular activity was abolished by docetaxel through the stabilization of microtubules, and by p38 MAPK inhibitor not only through the regulation of the p38 MAPK pathway, but also through the direct stabilization of microtubules, similar to docetaxel.

Microtubule (MT) homeostasis is governed by dynamic polymerization and depolymerization of the tubulin subunits. Since disrupting MT dynamics in cancer cells is thought to be useful for treating the tumor, numerous anti-

MT agents, such as vinca alkaloids and taxanes have been developed in the past quarter century. Although both vinca alkaloids and taxanes affect the MT, they have opposite modes of action; vinca alkaloids act by inhibiting the MT and the taxanes by stabilizing the MT (1-2). Acetylation of α -tubulin is a post-translational modification and is thought to be a marker for MT stability; acetylated α -tubulin is detected in stable MTs (3) and depolymerized tubulin is rapidly deacetylated *in vivo* (4). Thus, taxol, a MT-stabilizing agent, could induce an increase in the acetylation of α -tubulin (5). In addition, although anti-MT agents suppress the MT dynamics in cancer cells in common, only the MT-depolymerizing agents, but not the MT-stabilizing agents, specifically exert an antivascular activity against the tumor vascular endothelial cells in varying degrees (6, 7).

TZT-1027 (Soblidotin) is an MT-depolymerizing agent synthesized to have enhanced antitumor activity and reduced toxicity compared to dolastatin 10 (8, 9). The chemical structure of TZT-1027 is shown in Figure 1 (molecular weight, 701.98). TZT-1027 has been shown to inhibit strongly the growth of various human cancer cells *in vitro* (10), and its growth-inhibitory effect was less affected by overexpression of P-glycoprotein (P-gp) than that of other tubulin inhibitors and was not affected by overexpression of breast cancer resistance protein (BCRP) or multidrug resistance proteins (MRP) (11). In addition, TZT-1027 has been shown to exert antitumor activity against murine tumors and human xenografts (12). A significant inhibition of growth was observed when TZT-1027 was combined with CDDP, GEM and docetaxel in the A549 solid tumor model (13). Moreover, TZT-1027 has been recently verified to have antivascular activity *in vitro* and *in vivo* (14-16), like other vascular targeting agents (VTA), such as 5,6-dimethylxanthenone-4-acetic acid (DMXAA) (17) and combretastatin A-4 (CA4DP) (18). The antivascular activity of TZT-1027 has been evaluated in comparison with that of other anticancer agents, including MT-depolymerizing agents (vincristine, vinorelbine, CA4DP), an MT-stabilizing agent (docetaxel [DTX]), and non-MT binding agents (5-fluorouracil and cisplatin). TZT-

Correspondence to: Junichi Watanabe, ASKA Pharmaceutical Co. Ltd., Research and Development Division, 1604 Shimosakunobe, Takatsu-ku, Kawasaki-shi, Kanagawa 213-8522, Japan. Fax: +81 44 833 5310, e-mail: watanabe-j@aska-pharma.co.jp

Key Words: TZT-1027, Soblidotin, antivascular activity, p38 MAPK, HDAC6.

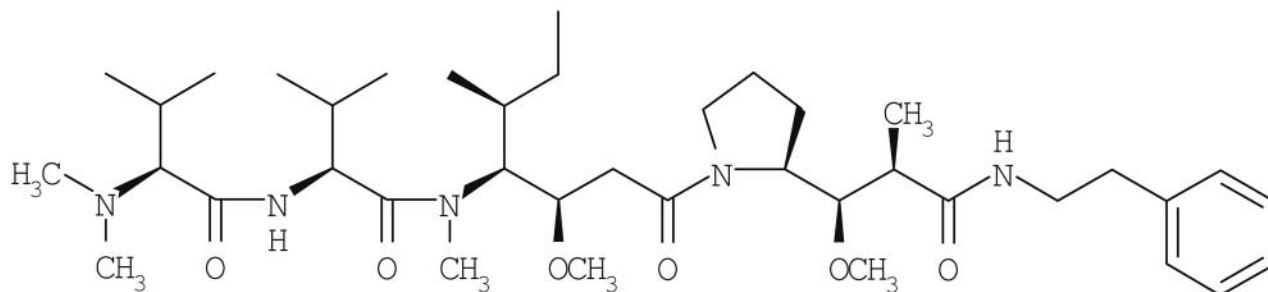


Figure 1. The chemical structure of TZT-1027.

1027 has been clearly shown to have potent antivasular activity, because of the ability to enhance the vascular permeability in human umbilical vein endothelial cells (HUVEC) monolayers and to reduce perfusion in advanced-stage Colon26 tumors implanted in mice, with efficacy superior to vinca alkaloids and comparable to CA4DP, a known VTA (19).

Disrupting the newly formed vasculature in the tumor is an attractive therapeutic strategy for solid tumors, because drug efficacy against the tumor vasculature would not be affected by drug resistance mechanisms in a wide variety of solid tumors. Although, for that reason, a number of VTA targeting the MT cytoskeleton in tumor vascular endothelial cells have been developed (17, 18), their mechanism of antivasular activity remains unclear (14). The aim of the present study was to elucidate the mechanism of the TZT-1027-induced antivasular activity by investigating the impact of various signal transduction inhibitors, including a p38 mitogen-activated protein kinase (MAPK) inhibitor (SB220025), a nitric oxide synthase (NOS) inhibitor (Nomega-nitro-L-arginine, L-NNA), Rho kinase inhibitors (Y-27632 and fasudil hydrochloride, Fasudil), an endothelin antagonist (SB209670), a 5-hydroxytryptamine (5-HT) antagonist (cyproheptadine, CYP), an MT-stabilizing agent (DTX), and a glucocorticoid (dexamethasone, DEX) on this activity. First, the inhibitory effects of various agents on TZT-1027-induced antivasular activity were screened *in vivo* by a tumor perfusion study in mice bearing advanced-stage Colon26 tumors, and subsequently, the ability of the agents that had an inhibitory effect in the *in vivo* study was verified *in vitro* by a vascular permeability study on HUVEC monolayer. Finally, Western blotting analyses of phosphorylated p38 MAPK and acetylated α -tubulin were performed to verify the mechanism of TZT-1027-induced antivasular activity.

Materials and Methods

Experimental animals and cell lines. Female BALB/c and CDF1 mice were purchased from Japan Charles River Co. Ltd. (Kanagawa, Japan). A murine adenocarcinoma cell line, Colon26,

was kindly supplied by the Cancer Chemotherapy Center, Japanese Foundation for Cancer Research (Tokyo, Japan) and maintained in syngeneic BALB/c mice in our laboratory. All animal experiments were conducted according to the Rules for the Care and Use of Laboratory Animals of ASKA Pharmaceutical Co., Ltd. HUVEC purchased from Cambrex (Walkersville, MD, USA), cultured in EGM-2 medium (EGM-2 Bullet Kit, Cambrex) and used for the experiments until passage 5. All cells were maintained at 37°C in the presence of 5% CO₂.

Drugs and reagents. TZT-1027, SB203580, SB209670, SB220025, Y-27632, and VX-745 were synthesized in our laboratory (Kanagawa, Japan). CYP and L-NNA were purchased from Sigma (St. Louis, MO, USA), Fasudil from Asahi Kasei (Tokyo, Japan), DTX from Aventis Pharma (Tokyo, Japan), and DEX from Nacalai Tesque, Inc. (Kyoto, Japan). In the *in vivo* study, TZT-1027 was dissolved in and diluted with 0.05 mol/L lactate buffer (pH 4.5), SB203580, SB209670, SB220025, Y-27632, and L-NNA were dissolved in and diluted with saline and CYP was dissolved in and diluted with distilled water. DEX was suspended in and diluted with saline, and preparations of Fasudil and DTX were diluted with saline. In the *in vitro* study, all of the agents were dissolved in and/or diluted with a medium appropriate for each experiment. Evans blue dye was purchased from PeptoTech EC Ltd. (London, UK), and fluorescein isothiocyanate (FITC)-dextran (70 kDa) from Sigma. Evans blue dye and FITC-dextran were dissolved in and diluted with saline and EBM medium (Cambrex), respectively.

Tumor perfusion study. Tumor blood volume was measured by the Evans blue dye perfusion technique, as described previously (14, 20, 21). Briefly, fragments (2 mm³) of Colon26 tumors were inoculated subcutaneously into the right flank of female CDF1 mice, and the experiment was performed when the tumor volume reached approximately 400 to 600 mm³. After pretreatment of mice bearing Colon26 with each agent or vehicle (saline), a single dose of 2 mg/kg TZT-1027 (14) or vehicle (lactate buffer) was administered intravenously at 10 mL/kg. The effective dose and administration route of each agent were as follows: SB209670 1 mg/kg, *i.v.* (22), Y-27632 30 mg/kg, *i.v.* maximum tolerated dose (MTD), Fasudil 30 mg/kg, *i.v.* MTD, CYP 20 mg/kg, *i.p.* (23), L-NNA 20 mg/kg, *i.v.* (24), and DTX 40 mg/kg, *i.v.* (25), all had 10 minutes of pretreatment. SB220025 50 mg/kg, *p.o.* (26) and DEX 0.1 mg/kg, *s.c.* (27) were administered 1 hour before TZT-1027. At 6 hours after administration of TZT-1027, 1% Evans blue dye was injected intravenously at 10 mL/kg. After 2 minutes, the mice were exsanguinated and sacrificed, and the tumor tissues were extirpated,

weighed and homogenized in a 5-fold volume of digestive solution [0.5% sodium sulfate-acetone (2:3)]. After incubation for 48 hours at room temperature to extract the Evans blue dye, the suspensions were centrifuged at 1,700xg for 10 minutes, and the amount of Evans blue dye in the supernatant was measured using a 96-well microplate reader (Nippon InterMed K.K., Tokyo, Japan) with absorbance set at 620 nm.

Gross findings. As in the tumor perfusion study, fragments (2 mm³) of Colon26 tumors were inoculated subcutaneously into the right flank of female CDF1 mice and the experiment was performed when the tumor volume reached approximately 400 to 600 mm³. At 1 hour after pretreatment of mice bearing Colon26 tumors with SB220025 (50 mg/kg, *p.o.*) or vehicle (saline), a single dose of 2 mg/kg TZT-1027 was administered intravenously at 10 mL/kg. At 1, 3, and 6 hours after administration of TZT-1027, the state of the tumor *in situ* in living mice and extirpated was observed grossly and photographed.

HUVEC monolayer permeability study. Diffusion of FITC-dextran passing through the HUVEC monolayer was determined as described previously (28, 29). Briefly, HUVEC were cultured on fibronectin-coated culture inserts (upper compartment, pore size: 3 μm) set on 24-well companion plates (lower compartment, Becton Dickinson, Bedford, MA, USA) containing EGM-2 medium at 2x10⁵ cells/well. When confluent monolayers were obtained after 2 days of culture, the two compartments were washed twice with PBS. DTX (10⁻⁷ g/mL), SB220025 (30 μM) and VX-745 (30 μM) diluted with EBM medium or the vehicle was added to the upper and lower compartments at 0.15 mL and 0.75 mL, respectively, for 30 minutes of pretreatment. SB220025 and VX-745 are p38 MAPK inhibitors with the same mechanism but differing in chemical structure were both used to ensure that any effect of SB220025 was not a non-specific inhibitory activity of SB220025 itself. After two washes with PBS, TZT-1027 (10⁻⁷ g/mL, a concentration which has been shown to significantly enhance vascular permeability (14)) in 0.15 mL diluted with 1 mg/mL FITC-dextran in EBM medium and the same concentration of TZT-1027 in 0.75 mL diluted with EBM medium was added to the upper and lower compartments, respectively. After 60 minutes of treatment, a 50-μL aliquot was sampled from the lower compartment, and its fluorescence intensity was measured (excitation: 490 nm; emission: 530 nm) using a 96-well microplate reader (Corona Electric Co., Ltd., Ibaragi, Japan).

Western immunoblot analysis. HUVEC were plated on a 90-mm dish at 2x10⁵ cells/mL. After 24 hours, they were treated with TZT (10⁻⁷ g/mL), DTX (10⁻⁷ g/mL), SB220025 (30 μM) or SB203580 (30 μM) diluted with EGM-2 medium. After treatment, HUVEC were washed with PBS and lysed with 0.2 mL SDS buffer (120 mM Tris-HCl, 4% SDS, pH 6.8). The lysate was centrifuged at 15,000xg for 5 minutes at 4°C, and the protein concentration of the supernatant was determined using a BCA Protein Assay Kit (PIERCE, Rockford, IL, USA). Equal amounts of protein (30 mg) were applied to an SDS-polyacrylamide gel, electrophoresed at 20 mA for 1 hour, transferred to a PVDF membrane (Millipore, Billerica, MA, USA) at 25 V for 1 hour, and subjected to immunoblot analysis. Detection was performed using an ECL Western blot detection system (Amersham Bioscience, Piscataway, NJ, USA), and the density of the band was scanned by an image scanner and quantified using the NIH image program (National Institutes of

Health, Bethesda, MD, USA). The primary antibodies for acetyl α -tubulin, β -tubulin, phospho-p38 (p-p38), and histone deacetylase 6 (HDAC6) were anti-acetyl α -tubulin monoclonal antibody (Sigma) anti- β -tubulin monoclonal antibody (Sigma), anti-p-p38 MAPK monoclonal antibody (Cell Signaling Technology, Danvers, MA, USA), and anti-HDAC6 antibody (Cell Signaling Technology), respectively. The secondary antibody for HDAC6 was anti-rabbit IgG horseradish peroxidase-linked whole antibody (Amersham Biosciences), the secondary antibody for the other primary antibodies was anti-mouse IgG horseradish peroxidase-linked whole antibody (Amersham Biosciences).

Statistical analyses. The data obtained from the tumor perfusion study and the HUVEC monolayer permeability study were analyzed using the parametric Student's *t*-test and the parametric Tukey type multiple comparison, respectively. Statistical analyses were carried out using SAS-system Release 8.2 software (SAS Institute Japan Ltd., Tokyo, Japan), and a *p*-value of less than 0.05 was considered statistically significant.

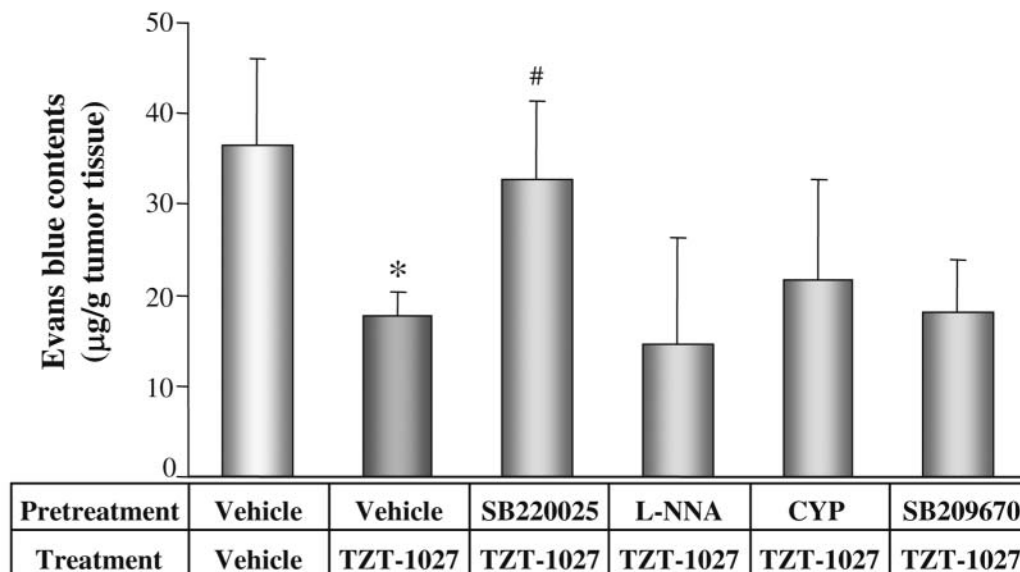
Results

Tumor perfusion study. The impact of the various signal transduction inhibitors on tumor perfusion is shown in Figure 2. Treatment with TZT-1027 for 6 hours significantly reduced tumor perfusion compared to vehicle alone, with Evans blue dye content decreasing from 36.6 to 17.6 μg/g (*p*<0.001) in experiment 1 and from 31.3 to 10.2 μg/g (*p*<0.001) in experiment 2. In addition, the TZT-1027-induced reduction of tumor perfusion was suppressed significantly by pretreatment with SB220025, but not with L-NNA, CYP or SB209670 and by pretreatment with DTX, but not with Y-27632, Fasudil, or DEX.

Gross findings. Whereas treatment with vehicle revealed little hemorrhage in the tumor (Figure 3a), treatment with TZT-1027 alone visibly caused irregular hemorrhage as early as 1 hour (Figure 3b), which became more marked with time (Figure 3c), and finally extended throughout the tumor 6 hours after administration (Figure 3d). In contrast, pretreatment with SB220025 attenuated the TZT-1027-induced hemorrhage compared to that with TZT-1027 alone 1 hour after administration of TZT-1027 (Figure 3e), with the tumor appearance almost similar to that with vehicle alone. In addition, although a slight hemorrhage was noted with SB220025 pretreatment 3 or more hours after administration of TZT-1027 (Figure 3f and Figure 3g), the degree of hemorrhage was less than that with TZT-1027 alone (Figure 3f and Figure 3g).

HUVEC monolayer permeability study. To clarify the antagonistic activity of DTX and SB220025, we next evaluated their effects on TZT-1027-induced increase in vascular permeability on a HUVEC monolayer (Figure 4 and Figure 5). Treatment with TZT-1027 significantly (*p*<0.001) increased

(A) Experiment 1



(B) Experiment 2

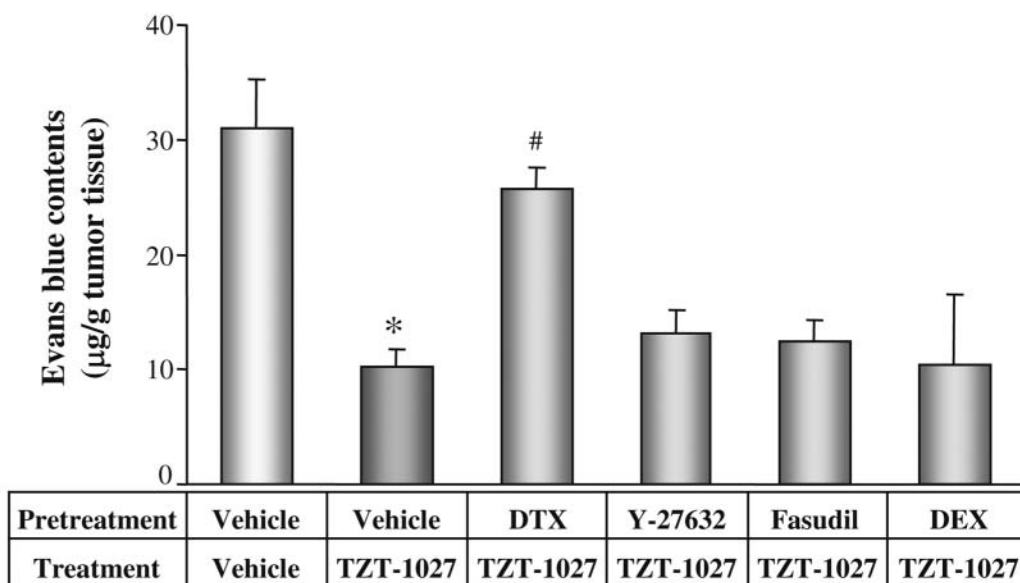


Figure 2. Inhibitory effect of various antitumor agents on TZT-1027-induced reduction of tumor perfusion in mice bearing Colon26 tumors. Pretreatment with SB220025 (a p38 MAPK inhibitor), L-NNA (a NOS inhibitor), CYP (a 5-HT antagonist) and SB209670 (an endothelin antagonist) in experiment 1 (A), as well as DTX (a MT-stabilizing agent), Y-27632 and Fasudil Rho kinase inhibitors and DEX (a glucocorticoid) in experiment 2 (B) was followed by treatment with TZT-1027 for 6 hours. Details in Materials and Methods. Tumor blood volume was determined spectrophotometrically using Evans blue dye. Each bar represents the mean \pm SD of 5 (experiment 1) or 8 (experiment 2) mice. * $p < 0.001$ versus (vehicle+vehicle) treated group; # $p < 0.001$ versus (vehicle+TZT-1027) treated group (Student's t-test).

the quantity of FITC-dextran passing through the HUVEC monolayer compared to the control in all three experiments (Figure 4, Figure 5A and Figure 5B), confirming a marked increase in vascular permeability. In contrast, pretreatment with DTX significantly ($p < 0.001$) suppressed the TZT-1027-induced increase in vascular permeability, with an inhibition rate (IR) of 86.0% (Figure 4). Pretreatment with SB220025 or

VX-745 significantly ($p < 0.001$) suppressed the TZT-1027-induced increase in vascular permeability, with IRs of 94.5% and 48.9%, respectively (Figure 5A and Figure 5B).

Western immunoblot analysis. The ability of TZT-1027 to induce the phosphorylation of p38 MAPK was investigated (Figure 6) (30-32). Although TZT-1027 induced the

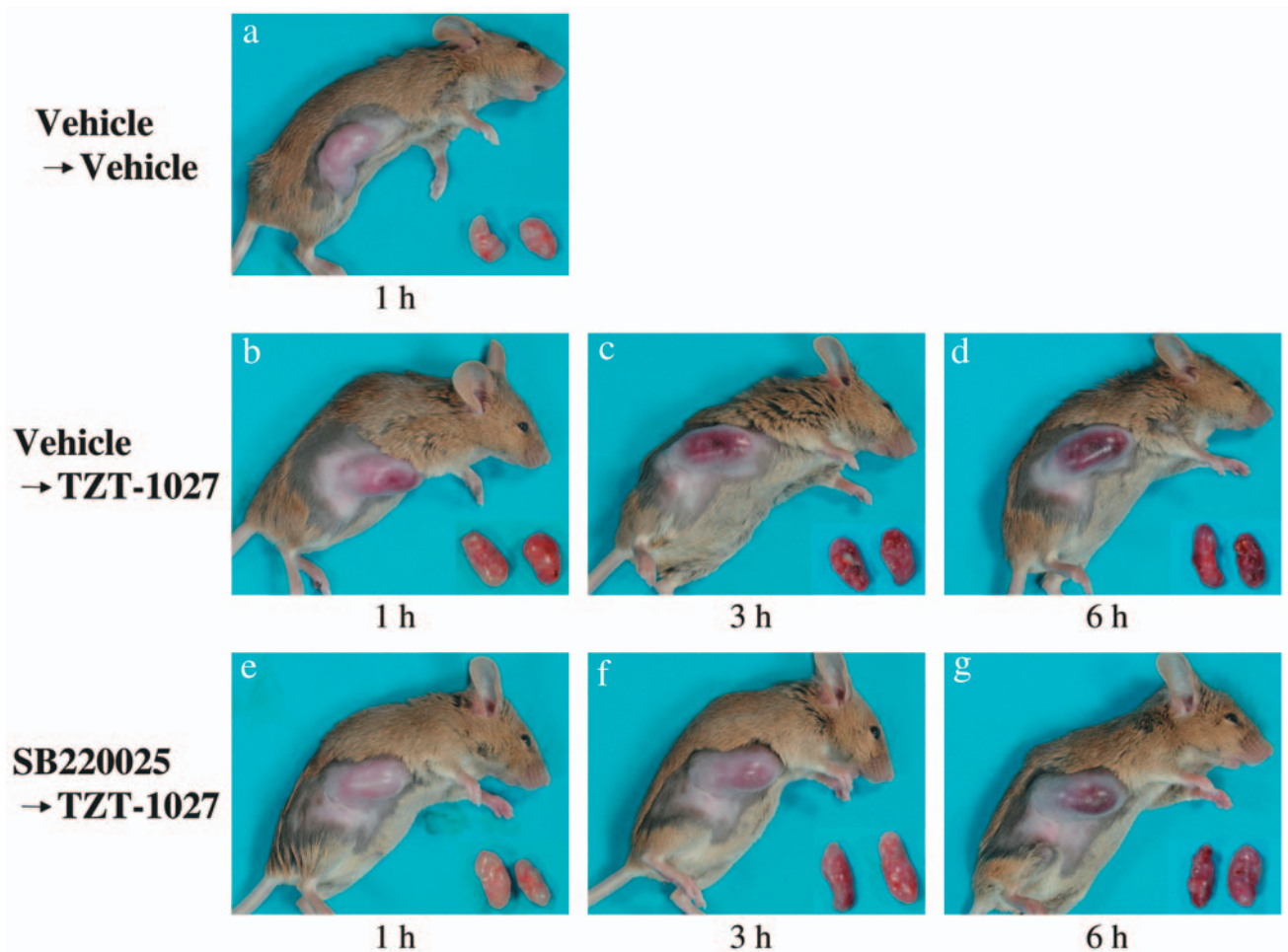


Figure 3. Effect of SB220025 on TZT-1027-induced hemorrhage in advanced-stage Colon26 tumors. At 1 hour after pretreatment of mice bearing Colon26 tumors with SB220025 (50 mg/kg, *p.o.*) or vehicle (saline), a single dose of 2 mg/kg TZT-1027 or lactate buffer was administered intravenously at 10 mL/kg. At 1, 3 and 6 hours after administration of TZT-1027, the state of the tumor *in situ* in living mice and extirpated was observed grossly and photographed.

phosphorylation of p38 MAPK in HUVEC after 30 minutes exposure, the expression level of phosphorylated p38 MAPK by TZT-1027 was markedly less than that by the positive control H_2O_2 (1 μ M, 5 min) (Figure 6A). Next, we examined whether TZT-1027 and DTX affected the acetylation of α -tubulin in HUVEC. Whereas TZT-1027 induced the deacetylation of α -tubulin from 5 minutes after treatment in a time-dependent manner, DTX conversely induced the acetylation of α -tubulin from 5 minutes after treatment an effect opposite to that of TZT-1027 (Figure 6B). Subsequently, we also examined the impact of the p38 MAPK inhibitors, SB220025 and SB203580, on acetylation of α -tubulin, and found that as with DTX both inhibitors induced an increase in acetylation of α -tubulin on HUVEC in a time-dependent manner, but had no effect on β -tubulin expression level (Figure 6B). Finally, we investigated the

expression level of HDAC6, which controls the deacetylation of MT (33), after treatment with TZT-1027, DTX, or SB220025 to clarify the involvement of HDAC6 in the p38 MAPK pathway and disruption of MT dynamics. No changes in the expression level of HDAC6 after 1 hour of treatment with TZT-1027, DTX or SB220025 were observed (Figure 6C).

Discussion

Previously, we demonstrated that TZT-1027 has antivascular activity, as do other VTAs, because it has the ability to induce the disruption of the MT cytoskeleton in vascular endothelial cells, the increase in vascular permeability in HUVEC monolayers and in tumors, the reduction of tumor perfusion, and tumoral hemorrhage (14). In the present

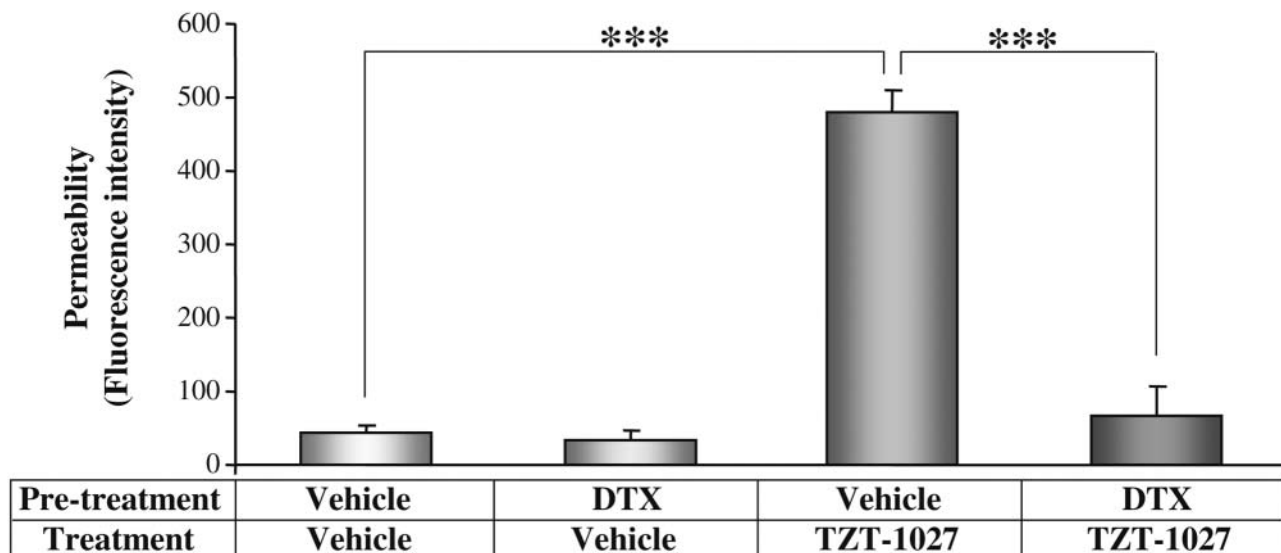


Figure 4. Inhibitory effect of MT-stabilizing agent, DTX, on TZT-1027-induced increase in vascular permeability on a HUVEC monolayer. Confluent endothelial monolayers grown on boyden chambers were pretreated with DTX (10^{-7} g/mL) or vehicle including FITC-dextran for 30 minutes and then treated with vehicle or TZT-1027 (10^{-7} g/mL) for 1 hour. Diffusion of FITC-dextran through the endothelial monolayer was determined by fluorescence microscopy. Each bar represents the mean \pm SD of three independent experiments. *** $p < 0.001$ (Parametric Tukey test).

study, among the agents examined, only a MT-stabilizing agent and a p38 MAPK inhibitor suppressed the TZT-1027-induced reduction of tumor perfusion (Figure 2), implying that disruption of the MT cytoskeleton would be necessary for the antivasular activity and that the p38 MAPK pathway might play an important role in the antivasular activity. The antagonistic activity was confirmed by an examination of their ability to attenuate TZT-1027-induced tumoral hemorrhage in the gross findings (Figure 3) and to suppress the TZT-1027-induced increase in vascular permeability (Figures 4 and 5). As an inhibitory effect was observed with both SB220025 and VX-745, the antagonistic activity on the TZT-1027-induced increase in vascular permeability was suggested to be common among p38 MAPK inhibitors. Previous data have suggested that the activation of the p38 MAPK pathway could cause a change in the endothelial actin cytoskeleton and an increase in vascular permeability on endothelial monolayers (30-32). In contrast, the Rho kinase inhibitors (Fasudil and Y-27632) only slightly inhibited the TZT-1027-induced reduction of tumor perfusion, although Rho kinase controls the rearrangement of actin microfilaments, one of the major components of the cytoskeleton, as well as the intermediate filaments and MTs. Our results supported the results of a previous report that an increase in vascular permeability is independent of Rho and Rho kinase activation, and indicated that the MT network, but not the actin network, may be an important modulator of endothelial barrier function leading to antivasular activity (34).

Acetylation of α -tubulin is closely involved in the stabilization of the MT cytoskeleton (3, 4). Paclitaxel, a MT-stabilizing agent like DTX, induced the acetylation of α -tubulin, and abolished the TNF- α -induced decrease in transendothelial electrical resistance (equal to an increase in vascular permeability) and the VTA (ZD6126)-induced MT depolymerization in HUVEC and acute necrosis in the tumor (4, 35, 36). As with previous reports, our results also showed that DTX markedly suppressed TZT-1027-induced antivasular activity in the reduction of tumor perfusion, the induction of tumor hemorrhage, and the increase in vascular permeability. We therefore suggest that VTA-induced antivasular activity would be suppressed commonly by MT-stabilizing agents, and importantly, by stabilizing the MTs (presented as an increase of acetylated α -tubulin), the opposite of VTA activity, which destabilizes the MTs (presented as a decrease of acetylated α -tubulin). The two anti-MT agents (TZT-1027, a MT-depolymerizing agent and DTX, a MT-stabilizing agent) appeared to have antagonistic effects at the level of the microtubule cytoskeleton.

Hydrogen peroxide has been suggested to activate the p38 MAPK pathway, followed by HUVEC permeability (32), but unexpectedly, TZT-1027 did not increase the expression level of phosphorylated p38 MAPK as much as the positive control, H_2O_2 . Additionally the onset of phosphorylation of p38 MAPK was delayed in comparison with the increase in vascular permeability, which occurred as early as 15 minutes after treatment with TZT-1027 (16).

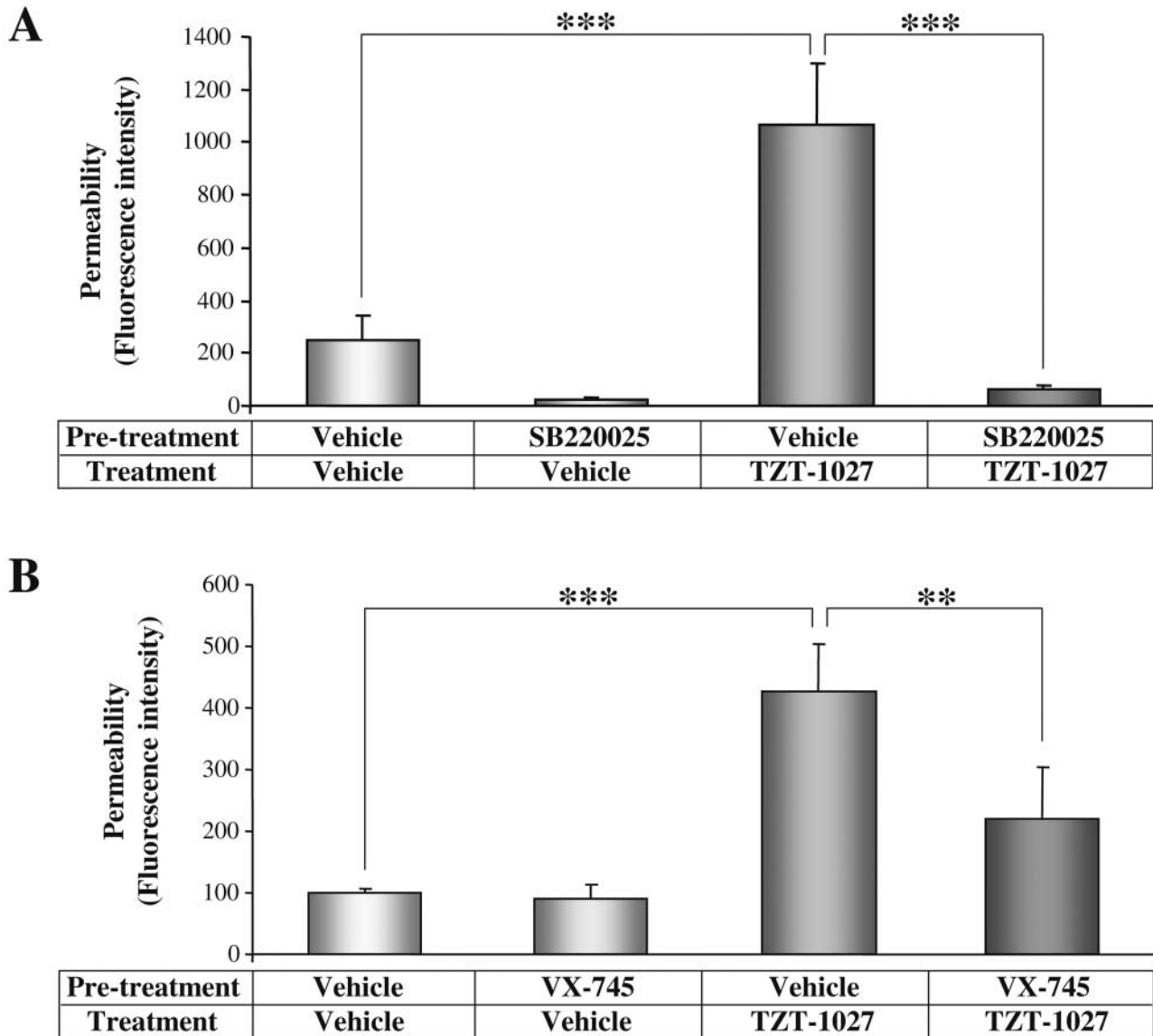


Figure 5. Inhibitory effect of p38 MAPK inhibitors, SB220025 (A) and VX-745 (B) on TZT-1027-induced increase in vascular permeability on the HUVEC monolayer. Confluent endothelial monolayers grown on boyden chambers were pretreated with SB220025 (10^{-7} g/mL), VX-745 (10^{-7} g/mL) or vehicle including FITC-dextran for 30 minutes and then treated with vehicle or TZT-1027 (10^{-7} g/mL) for 1 hour. Diffusion of FITC-dextran through the endothelial monolayer was determined by fluorescence microscopy. Each bar represents the mean \pm SD of three independent experiments. ** $p < 0.01$ *** $p < 0.001$ (Parametric Tukey test).

Moreover, although the inhibition of p38 MAPK by SB203580 suppressed CA4DP-induced membrane blebbing in HUVEC, CA4DP itself rarely induced the phosphorylation of p38 MAPK. Taken together, these data indicated that involvement of the p38 MAPK pathway is minimal in the antivascular activity of VTAs and that p38 MAPK inhibitors would exert their activity *via* another mechanism. Additionally, like DTX the p38 MAPK inhibitors also induced α -tubulin acetylation. This novel

finding suggested the possibility that p38 MAPK inhibitors would abolish the TZT-1027-induced antivascular activity not only through the regulation of the p38 MAPK pathway, but also through the direct stabilization of the MT cytoskeleton.

TNF- α , which triggers MT disassembly and has antivascular activity like TZT-1027, also induced an increase in vascular permeability and a decrease in stable tubulin content (35, 37, 38). In addition, inhibition of p38 MAPK

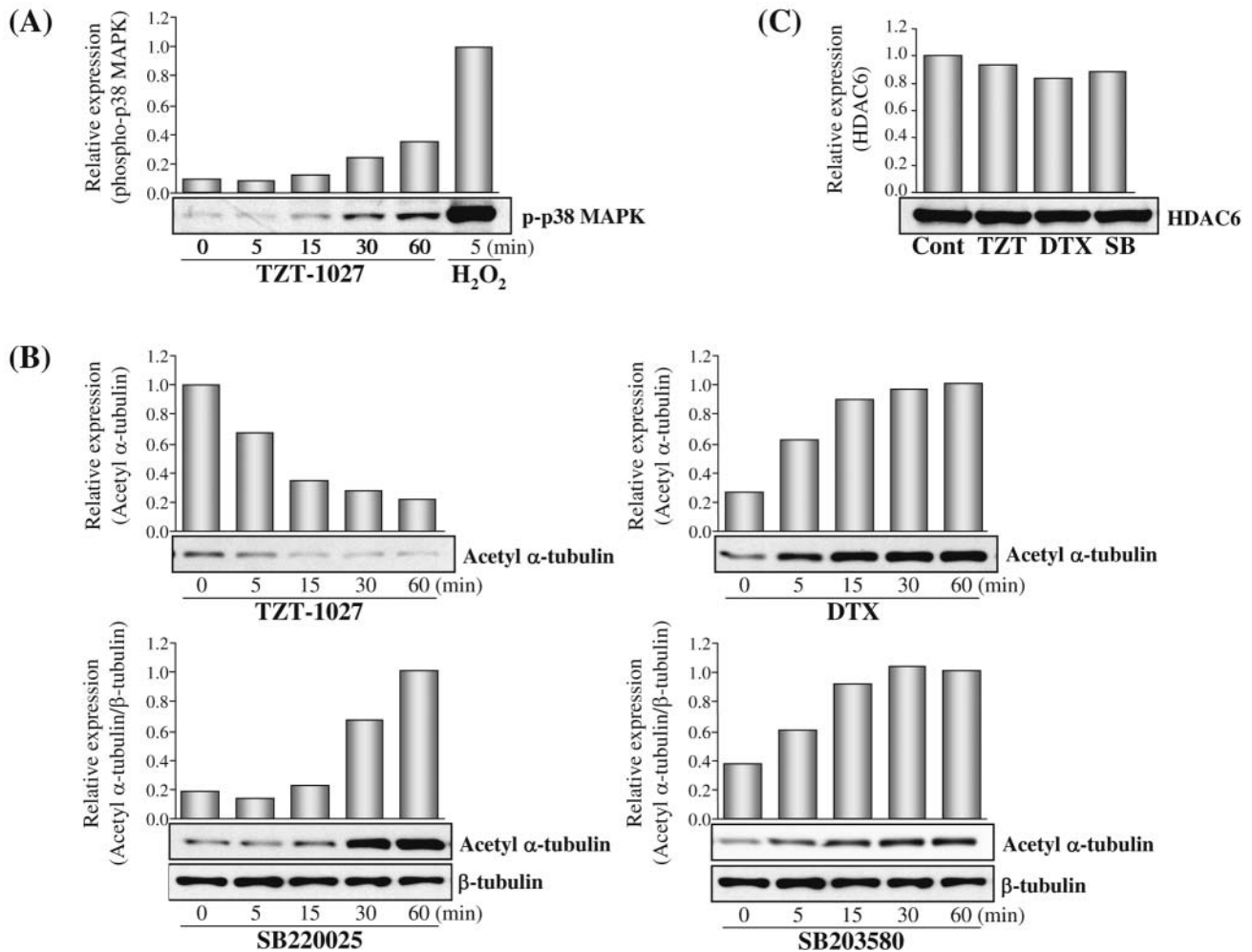


Figure 6. The impact of TZT, DTX, SB220025 and SB203580 on expression levels of phospho-p38 MAPK (A), acetyl α -tubulin (B) and HDAC6 (C). HUVEC were treated with TZT-1027 (10^{-7} g/mL), DTX (10^{-7} g/mL), SB220025 ($30 \mu\text{M}$), or SB203580 ($30 \mu\text{M}$). Expression levels were detected using Western blot analysis, and the density of the band was scanned by an image scanner and quantified using the NIH image program. H₂O₂: Hydrogen peroxide; TZT: TZT-1027; SB: SB220025.

by SB203580 significantly attenuated TNF- α -induced MT polymerization, actin rearrangement and endothelial barrier dysfunction (35). Although these results strongly suggest the involvement of MT rearrangement in TNF- α -induced endothelial cell permeability *via* p38 MAPK activation, the exact mechanism by which TNF- α triggers vascular barrier dysfunction has not been precisely defined (35). However, in this study, our novel findings suggested that as well as DTX, the p38 MAPK inhibitors could play a major role in antagonistic activity to TZT-1027 through the stabilization of MTs. The antagonistic activity of p38 MAPK inhibitors on CA4DP and TNF- α is also considered to be attributable to stabilization of the MTs. Finally, we investigated whether TZT-1027, DTX, or SB220025 affected the expression level of HDAC6, since HDAC6 controls the deacetylation of α -tubulin and inhibition of HDAC6 by trichostatin A leading

to an increase in acetylated α -tubulin (33, 39). Although there were no changes in the expression level of HDAC6, further examination to investigate the localization and activation of HDAC6 would be necessary to clarify the involvement of HDAC6 in antivascular activity. Moreover, we believe that elucidating the mechanism of interaction among MT dynamics, acetylation/deacetylation of α -tubulin, activation/inactivation of HDAC6 and the p38 MAPK pathway will play an important role in the treatment of solid tumors through antivascular activity.

In conclusion, the presented results suggest that TZT-1027-induced antivascular activity was abolished by DTX through the stabilization of microtubules, and by p38 MAPK inhibitors not only through the regulation of the p38 MAPK pathway, but also through the direct stabilization of microtubules, similar to DTX.

References

- 1 Wilson L: Microtubules as drug receptors: pharmacological properties of microtubule protein. *Ann N Y Acad Sci* 253: 213-231, 1975.
- 2 Schiff PB and Horwitz SB: Taxol stabilizes microtubules in mouse fibroblast cells. *Proc Natl Acad Sci USA* 77: 1561-1565, 1980.
- 3 Schulze E, Asai DJ, Bulinski JC and Kirschner M: Posttranslational modification and microtubule stability. *J Cell Biol* 105: 2167-2177, 1987.
- 4 Matsuyama A, Shimazu T, Sumida Y, Saito A, Yoshimatsu Y, Seigneurin-Berny D, Osada H, Komatsu Y, Nishino N, Khochbin S, Horinouchi S and Yoshida M: *In vivo* destabilization of dynamic microtubules by HDAC6-mediated deacetylation. *EMBO J* 21: 6820-6831, 2002.
- 5 Piperno G, LeDizet M and Chang XJ: Microtubules containing acetylated alpha-tubulin in mammalian cells in culture. *J Cell Biol* 104: 289-302, 1987.
- 6 Tozer GM, Kanthou C, Parkins CS and Hill SA: The biology of the combretastatins as tumour vascular targeting agents. *Int J Exp Pathol* 83: 21-38, 2002.
- 7 Jordan MA and Wilson L: Microtubules as a target for anticancer drugs. *Nat Rev Cancer* 4: 253-265, 2004.
- 8 Miyazaki K, Kobayashi M, Natsume T, Gondo M, Mikami T, Sakakibara K and Tsukagoshi S: Synthesis and antitumor activity of novel dolastatin 10 analogs. *Chem Pharm Bull* 43: 1706-1718, 1995.
- 9 Natsume T, Watanabe J, Tamaoki S, Fujio N, Miyasaka K and Kobayashi M: Characterization of the interaction of TZT-1027, a potent antitumor agent with tubulin. *Jpn J Cancer Res* 91: 737-747, 2000.
- 10 Watanabe J, Natsume T, Fujio N, Miyasaka K and Kobayashi M: Induction of apoptosis in human cancer cells by TZT-1027, an antimicrotubule agent. *Apoptosis* 5: 245-253, 2000.
- 11 Watanabe J, Minami M and Kobayashi M: Antitumor activity of TZT-1027 (Soblidotin). *Anticancer Res* 26: 1973-1981, 2006.
- 12 Kobayashi M, Natsume T, Tamaoki S, Watanabe J, Asano H, Mikami T, Miyasaka K, Miyazaki K, Gondo M, Sakakibara K and Tsukagoshi S: Antitumor activity of TZT-1027, a novel dolastatin 10 derivative. *Jpn J Cancer Res* 88: 316-327, 1997.
- 13 Natsume T, Watanabe J, Horiuchi T and Kobayashi M: Combination effect of TZT-1027 (Soblidotin) with other anticancer drugs. *Anticancer Res* 26: 1145-1151, 2006.
- 14 Watanabe J, Natsume T and Kobayashi M: Anti-vascular effects of TZT-1027 (Soblidotin) on murine Colon26 adenocarcinoma. *Cancer Sci* 97: 1410-1416, 2006.
- 15 Otani M, Natsume T, Watanabe J, Kobayashi M, Murakoshi M, Mikami T and Nakayama T: TZT-1027, an antimicrotubule agent, attacks tumor vasculature and induces tumor cell death. *Jpn J Cancer Res* 91: 837-844, 2000.
- 16 Natsume T, Watanabe J, Ogawa K, Yasumura K and Kobayashi M: Tumor-specific antivasular effect of TZT-1027 (Soblidotin) elucidated by magnetic resonance imaging and confocal laser scanning microscopy. *Cancer Sci* 98: 598-604, 2007.
- 17 Philpott M, Baguley BC and Ching LM: Induction of tumour necrosis factor-alpha by single and repeated doses of the antitumour agent 5, 6-dimethylxanthenone-4-acetic acid. *Cancer Chemother Pharmacol* 36: 143-148, 1995.
- 18 Dark GG, Hill SA, Prise VE, Tozer GM, Pettit GR and Chaplin DJ: Combretastatin A-4, an agent that displays potent and selective toxicity toward tumor vasculature. *Cancer Res* 57: 1829-1834, 1997.
- 19 Watanabe J, Natsume T and Kobayashi M: Comparison of the antivasular and cytotoxic activities of TZT-1027 (Soblidotin) with those of other anticancer agents. *Anticancer Drugs*, in press, 2007.
- 20 Bibby MC, Double JA, Loadman PM and Duke CV: Reduction of tumor blood flow by flavone acetic acid: a possible component of therapy. *J Natl Cancer Inst* 81: 216-220, 1989.
- 21 Laws AL, Matthew AM, Double JA and Bibby MC: Preclinical *in vitro* and *in vivo* activity of 5,6-dimethylxanthenone-4-acetic acid. *Br J Cancer* 71: 1204-1209, 1995.
- 22 Maki S, Miyauchi T, Sakai S, Kobayashi T, Maeda S, Takata Y, Sugiyama F, Fukamizu A, Murakami K, Goto K and Sugishita Y: Endothelin-1 expression in hearts of transgenic hypertensive mice overexpressing angiotensin II. *J Cardiovasc Pharmacol* 31: 412-416, 1998.
- 23 Milson JA and Pycock CJ: Effects of drugs acting on cerebral 5-hydroxytryptamine mechanisms on dopamine-dependent turning behaviour in mice. *Br J Pharmacol* 56: 77-85, 1976.
- 24 Gabra BH and Sirois P: Pathways for the bradykinin B1 receptor-mediated diabetic hyperalgesia in mice. *Inflamm Res* 53: 653-657, 2004.
- 25 Hashiguchi N, Kubota T, Koh J, Yamada Y, Saikawa Y, Otani Y, Watanabe M, Kumai K, Kitajima M, Watanabe J and Kobayashi M: TZT-1027 elucidates antitumor activity through direct cytotoxicity and selective blockade of blood supply. *Anticancer Res* 24: 2201-2208, 2004.
- 26 Lal BK, Varma S, Pappas PJ, Hobson RW II and Duran WN: VEGF increases permeability of the endothelial cell monolayer by activation of PKB/akt, endothelial nitric-oxide synthase, and MAP kinase pathways. *Microvasc Res* 62: 252-262, 2001.
- 27 Kanthou C and Tozer GM: The tumor vascular targeting agent combretastatin A-4-phosphate induces reorganization of the actin cytoskeleton and early membrane blebbing in human endothelial cells. *Blood* 99: 2060-2069, 2002.
- 28 Jackson JR, Bolognese B, Hillegass L, Kassis S, Adams J, Griswold DE and Winkler JD: Pharmacological effects of SB 220025, a selective inhibitor of P38 mitogen-activated protein kinase, in angiogenesis and chronic inflammatory disease models. *J Pharmacol Exp Ther* 284: 687-692, 1998.
- 29 Oyanagui Y: Natural antioxidants enhance and prolong the oxyradical/no-related suppression by dexamethasone of ischemic and histamine paw edema in mice. *Inflammation* 21: 643-654, 1997.
- 30 Huot J, Houle F, Marceau F and Landry J: Oxidative stress-induced actin reorganization mediated by the p38 mitogen-activated protein kinase/heat shock protein 27 pathway in vascular endothelial cells. *Circ Res* 80: 383-392, 1997.
- 31 Rousseau S, Houle F, Landry J and Huot J: p38 MAP kinase activation by vascular endothelial growth factor mediates actin reorganization and cell migration in human endothelial cells. *Oncogene* 15: 2169-2177, 1997.
- 32 Kevil CG, Oshima T and Alexander JS: The role of p38 MAP kinase in hydrogen peroxide mediated endothelial solute permeability. *Endothelium* 8: 107-116, 2001.
- 33 Hubbert C, Guardiola A, Shao R, Kawaguchi Y, Ito A, Nixon A, Yoshida M, Wang XF and Yao TP: HDAC6 is a microtubule-associated deacetylase. *Nature* 417: 455-458, 2002.

- 34 Petrache I, Verin AD, Crow MT, Birukova A, Liu F and Garcia JG: Differential effect of MLC kinase in TNF-alpha-induced endothelial cell apoptosis and barrier dysfunction. *Am J Physiol Lung Cell Mol Physiol* 280: 1168-1178, 2001.
- 35 Petrache I, Birukova A, Ramirez SI, Garcia JG and Verin AD: The role of the microtubules in tumor necrosis factor-alpha-induced endothelial cell permeability. *Am J Respir Cell Mol Biol* 28: 574-581, 2003.
- 36 Taraboletti G, Micheletti G, Dossi R, Borsotti P, Martinelli M, Fiordaliso F, Ryan AJ and Giavazzi R: Potential antagonism of tubulin-binding anticancer agents in combination therapies. *Clin Cancer Res* 11: 2720-2726, 2005.
- 37 Molony L and Armstrong L: Cytoskeletal reorganizations in human umbilical vein endothelial cells as a result of cytokine exposure. *Exp Cell Res* 196: 40-48, 1991.
- 38 Mahadevan V, Malik ST, Meager A, Fiers W, Lewis GP and Hart IR: Role of tumor necrosis factor in flavone acetic acid-induced tumor vasculature shutdown. *Cancer Res* 50: 5537-5542, 1990.
- 39 Dowdy SC, Jiang S, Zhou XC, Hou X, Jin F, Podratz KC and Jiang SW: Histone deacetylase inhibitors and paclitaxel cause synergistic effects on apoptosis and microtubule stabilization in papillary serous endometrial cancer cells. *Mol Cancer Ther* 5: 2767-2776, 2006.

Received May 24, 2007

Revised July 24, 2007

Accepted August 8, 2007